Lawrence Berkeley National Laboratory

Title
PHOTOELECTRON DIFFRACTION MEASUREMENTS OF SULFUR AND SELENIUM ADSORBED ON Ni(OOl)

Permalink
https://escholarship.org/uc/item/0w3199gg

Author
Kevan, S.D.

Publication Date
1979-04-01

LBL-9024
Preprint

PHOTOELECTRON DIFFRACTION MEASUREMENTS OF SULFUR AND SELENIUM ADSORBED ON Ni(001)

S. D. Kevan, D. H. Rosenblatt, D. R. Denley,
B.-C. Lu, and D. A. Shirley

April 1979

DISCLAIMER

PHOTOELECTRON DIFFRACTION MEASUREMENTS OF
SULFUR AND SELENIUM ADSORBED ON Ni(001)

S. D. Kevan, D. H. Rosenblatt, D. R. Denley,*
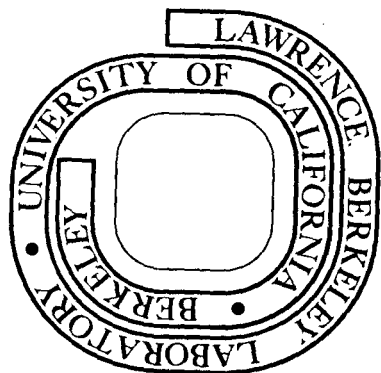B.-C. Lu, and D. A. Shirley

Materials and Molecular Research Division
Lawrence Berkeley Laboratory
and
Department of Chemistry
University of California
Berkeley, California 94720

April 1979

ABSTRACT

Photoelectron diffraction data are presented for the systems
sulfur/Ni(001) and selenium/Ni(001). A combination of all normal
emission data leads to a clearer understanding of photoelectron
diffraction from an adsorbate core level as a two-step process.
Experimental observation of diffraction effects from low coverage,
disordered overlayers of selenium demonstrates that the diffrac-
tion is clearly due to backscattering off the nickel substrate,
and also that normal photoelectron diffraction is potentially
quite useful in the study of disordered systems. Certain criteria
are established which any photoelectron diffraction technique
must satisfy to be a viable tool for studying surface structure.
A comparison of c(2x2) sulfur and selenium data and presentation
of off-normal data for the selenium system leads to the conclu-
sion that normal photoelectron diffraction satisfies these cri-
teria. Normal photoelectron diffraction was observed for the
nickel 3p shell and valence band, showing that both diffraction

*Also with the Dept. of Physics, University of Calif., Berkeley.

and multiple scattering processes affect angle-resolved photo-

emission intensities.

I.   INTRODUCTION

The possible use of final-state scattering effects in angle-resolved photoemission from adsorbate orbitals to determine adsorbate-surface structure has been the subject of several recent theoretical investigations.[1,2] The basic idea is that the photoelectron's de Broglie wavelength would be comparable to interatomic distances, leading to diffraction phenomena. Photoelectron diffraction has recently been observed in several systems, in two experimental modes: normal and azimuthal photoelectron diffraction. In normal photoelectron diffraction (NPD),[3,4] energy-analyzed photoelectrons from a specific adsorbate level are collected in "normal" geometry; i.e., perpendicular to the substrate surface. The photon energy is swept through a wide range, and an electron intensity-vs-energy curve is thereby generated. Azimuthal photoelectron diffraction (APD)[5,6] consists of rotating the sample about its normal and recording the intensity of the energy-analyzed adsorbate core-level photoelectron peak, while holding the photon energy constant. Both NPD and APD have some experimental advantages, but neither has as yet been shown to be a generally useful technique for adsorbate structure determinations, although in an earlier study[3] we inferred that this might well be the case for NPD. In this paper we shall present further evidence which indicates that NPD is in fact of general applicability. In the course of the paper we shall answer several questions that were left open before.

In our earlier study,[3] normal photoelectron diffraction was
observed in the c(2x2) Se/Ni(001) system. Remarkably good agree-
ment was found between peak positions in the Se(3d) intensity
measured normal to the surface as a function of photon energy
and recent calculations by Tong and Li.[2] The data supported
conclusions from LEED[7] that selenium sits in a fourfold hollow
site on Ni(001). However, we also noted an equally remarkable
correspondence of the peak positions to those observed in the
LEED 00 beam. If the Tong-Li calculations had not been avail-
able, our results might have been interpreted as indicating
that NPD measures essentially the LEED 00 beam. These two
observations actually lead to contradictory conclusions: the
LEED 00 beam peak positions are often quite insensitive to the
adsorbate-substrate interplanar spacing, $d_\perp$, while $d_\perp$ was in
fact the crucial parameter in the Tong-Li calculations.

Recent azimuthal studies, on the other hand, have also not
definitively shown APD to be sensitive to $d_\perp$. Indeed calcula-
tions by Tong and Li on the Se/Ni(001) system tend to show that,
for this system at least, the azimuthal studies are not very
sensitive to $d_\perp$. Scattering mechanisms within the adsorbate
overlayer itself are emphasized, and essentially the same azi-
muthal variations of intensity were obtained, independent of
$d_\perp$.[8a] However other calculations[8b] indicate that pronounced
variations in the azimuthal dependence on $d_\perp$ are present for
selected kinetic energies. We leave the subject of APD at this
point, noting that more work is needed to establish the magnitude

of its sensitivity to $d_\perp$.

Clearly, any photoelectron diffraction technique must satisfy at least two closely-related criteria before becoming a viable method for adsorbate structure determination. First, the dominant scattering process must be off the substrate, and must manifest itself as easily measureable variations in differential cross-section. Second, the mechanism must be sensitive to adsorbate registry through $d_\perp$ or some other useful parameter. In this paper we describe experiments designed to test the extent to which NPD does indeed satisfy both of these requirements.

In Section II we outline the experimental techniques more explicitly than in our previous paper.[3] Section III presents new photoelectron diffraction data from a series of experiments which answer specific questions about the promise of NPD as a surface structural tool. Conclusions are summarized in Section IV.

II. EXPERIMENTAL

All the experiments were performed on the 4° branch of Beam Line I at the Stanford Synchrotron Radiation Laboratory (SSRL). On this line, usable photon intensities are available between 40 and 280 eV photon energy. The photoelectron spectrometer employs a 5.40 cm mean radius hemispherical analyzer which can be rotated through 2π steradians of solid angle and which allows for simultaneous analysis of a range of electron

kinetic energies via a resistive anode multichannel detection system, thereby enhancing the detection sensitivity by a factor usually between 10 and 100. This latter feature was especially important in the studies reported here, as the ring current was quite low (3-4 mA) throughout our running time, yielding a proportionally low photon flux. In fact these experiments would have been impossible with a single-channel detection system. A more complete description of the analyzer, drive, and detection system will be published in the near future.

A high-purity nickel single crystal with a surface orientation to within 1° of the (001) face was mounted in the photo-emission spectrometer. Previous treatment of the crystal had largely removed the bulk impurities, so that short cycles of argon-ion bombardment and annealing to 700°C were sufficient to produce a clean and ordered surface as determined by in situ LEED/Auger analysis. Selenium and sulfur coverages were prepared by directing an effusive beam of H_2Se or H_2S at the crystal, which was heated to 200°C. Exposures roughly equivalent to those reported by Hagstrom and Becker[9] were required to produce ordered c(2x2) overlayers. Low-resolution energy distribution curves of the appropriate adsorbate core level (Se(3d) or S(2p)) were recorded at photon-energy increments of 3 eV. Figure 1 shows part of the photoelectron spectrum of c(2x2) Se/Ni(001) at a photon energy hν = 150 eV. The nickel valence band and 3p peak are clearly visible, as is the Se 3d peak. The surface sensitivity of NPD is exemplified by the fact that this latter

peak, which arises from a half-monolayer adsorbate coverage, is of comparable intensity to the bulk-derived nickel peaks. On comparing a series of spectra like that in Fig. 1, but taken at successive photon energies, dramatic variations in the relative intensities of these three peaks were obvious by visual inspection — a convincing demonstration of photoelectron diffraction. To obtain peak intensities, a smooth background was subtracted from the electron distribution curves, the peak areas were calculated, and corrections were made for photon flux and analyzer transmission. These corrections are discussed below.

In constant-initial-state (CIS) photoelectron spectroscopy the excitation of a given core level of binding energy E_B is followed by varying the kinetic energy (KE) at which the photoelectrons are collected to satisfy the Einstein relation

$$E_B = h\nu - KE$$

In all CIS studies two corrections are obligatory at each $(h\nu, KE)$ combination. The first is a correction for the analyzer transmission function which, from elementary optics, goes as $(KE)^{-1}$.[10] This form of the correction, which should be a good approximation for our analyzer, has now been applied. In any case, the correction is smooth and will not affect peak positions significantly. The second correction, that of correcting for incident photon flux, is more troublesome, because VUV monochromator transmission functions are far from

smooth. In this work and in our previous study[3] we have cor-
rected for photon flux by measuring the photoyield from a gold
mesh and assuming that the observed photoyield is proportional
to the gold absorption coefficients measured by Hagemann, et al.[11]
The similarity of the transmission thus determined to that
measured earlier with a standardized Al_2O_3 photodiode[12] indi-
cates that this assumption is reasonable and that at most any
discrepancies vary slowly with energy. The advantage of using
a gold mesh is that photoyield measurements can usually be
made simultaneously with the photoemission experiments, although
the low beam currents mentioned above precluded doing so in the
present work. Instead, the photoyield measurements were carried
out before the photoemission measurements and appropriate cor-
rections for beam current were made later. A plot of the
resulting corrected intensities produces essentially a constant-
initial state photoemission spectrum. In all cases background
subtraction near 62 eV kinetic energy was complicated by a
broad nickel Auger peak at this energy. Hence, data near this
kinetic energy should be treated with caution.

III. RESULTS AND DISCUSSION

In this Section we present the results of a series of
experiments. Each is discussed in turn, and conclusions are
summarized in Section IV.

Proceeding from the spectra presented in Fig. 1, it is
natural to inquire whether the nickel 3p and valence-band peaks

exhibit photoelectron diffraction, in addition to that shown
by the Se(3d) peaks, which was documented previously.[3] They
do, indeed. Figure 2 shows the intensity variation of the
nickel-derived features, plotted against energy. Peak positions
for the Se p(2x2) structure lie at the following kinetic ener-
gies (relative to the nickel vacuum level): Ni(3p); 54, 73, 111,
145 eV; Ni(valence band); 82, 119, 187 eV. We present these
results simply to document the effect of photoelectron diffrac-
tion from substrate-derived peaks, and will make no attempt at
quantitative data reduction. The fact that intensity maxima
lie at different kinetic energies for the Se(3d), Ni(3d), and
Ni(3p) shells is noteworthy, and it suggests several future
lines of investigation, but no unique interpretation. Obviously
the nickel data are less amenable to simple interpretation than
those from the Se(3d) orbitals, because the photo-current ori-
ginates from several inequivalent layers of lattice atoms. It
should be noted that photoelectron diffraction can substantially
modulate angle-resolved photoelectron (ARP) intensities from
single crystals, at the ±30% level. Thus ARP intensity varia-
tions cannot be interpreted meaningfully at a higher level of
accuracy unless photoelectron diffraction has been taken into
account.

Figure 3 shows all of our NPD results on the c(2x2) Se/Ni
(001) system obtained to date. The top curve repeats our
earlier data,[3] after an error that was made in correcting for
the analyzer transmission function in the earlier study has

been removed. This gives a significant change in relative peak intensities, but peak positions, which are listed in Table I for all four curves, have changed by at most 1-2 eV. Curves b, c, and d in Fig. 3 show new data on this system. Curve b was obtained under the same conditions as curve a, and shows remarkably consistent results. Peak positions are identical to within 1-2 eV, and the peak intensities are nearly the same. Curve c demonstrates the effect of changing the angle of incidence of the light to 80° along the same [100] azimuth, so that the $\vec{A}$ vector is only 10° off normal. There is a small shift in peak positions and intensities. Finally, curve d shows the effect of changing the azimuthal incidence of the light to be along the [110] azimuth. We conclude that, at the level of accuracy with which the NPD curves in Fig. 3 were measured, the peak positions and intensities are quite reproducible and do not depend sensitively on the azimuthal or polar orientation of the photon polarization vector in the range that we have studied.

At this point a preliminary estimate of the accuracy of $d_\perp$ values determined by NPD is of interest. This estimate must be preliminary because only a very limited set of data and of theoretical curves is available. For the same reason it must be conservative. We note the rms peak-energy reproducibility of ±1.5 eV in Table I and the rms shift of 50 eV/Å in the peak positions calculated by Tong and Li (cited in Ref. 3) between the twofold bridge and fourfold hollow-site peak positions. Division yields ±0.03Å: on this basis it is realistic

to estimate the error of NPD as $\pm 0.05\text{Å}$ in $d_\perp$, which compares with LEED accuracies.

There is another pleasing common characteristic of the four curves in Fig. 3. If the diffraction maxima and minima could be eliminated by some sort of averaging process, the remaining curves would have the energy dependence expected tor a nodeless initial state. That is, the intensity would rise above threshold to a broad maximum centered about 100 eV above threshold, then decrease. This observation, which was missed in the earlier study[3] because of the errant correction for analyzer transmission, supports the view of photoelectron diffraction as a two-step process. There is first an atomic-like excitation followed by scattering in the final state which introduces intensity oscillations with energy. The photoemit-ting atom acts like an electron gun, with an "emission current" given by the atomic cross-section. The observed photoemission intensity can then be taken as a product of an atomic cross-section term and an oscillatory function which describes the final-state scattering. This picture is consistent with recent theoretical predictions[13] that initial states possessing radial nodes exhibit NPD curves with one major sharp peak, the position of which is insensitive to $d_\perp$. The peak is merely an artifact of a Cooper minimum in the atomic cross-section, which sharply attenuates the cross-section a few eV above threshold, and keeps it at a low value for a long range of energy. Although the diffraction oscillations may be present at higher energies

they will be difficult to observe because the entire elastic peak in the photoemission spectrum is very weak and is obscured by "noise" arising from the inelastic background.

At this point we make an interesting qualitative comparison of the NPD spectrum for the p(2x2)Se/Ni(001) system to the published[14] LEED 00 and 01 beams for this system, as well as to the curve calculated by Tong and Li. We commented briefly on this comparison before. All four curves appear in Fig. 4. The close correspondence of peak positions is striking, and it supports the prediction that an NPD spectrum should contain a coherent superposition of LEED beams, with the normal 00 beam being emphasized in the NPD spectrum. As noted before,[3] the peaks at ca. 37, 88, and 134 eV are Bragg peaks in the 00 beam, while the 58 eV peak arises from multiple scattering, thereby demonstrating the importance of considering multiple scattering in angle-resolved photoemission. Another earlier observation — that the NPD relative peak intensities were close to those in the 00 LEED beam — was incorrect in light of the new intensity corrections.

To further characterize constant-initial-state photoelectron diffraction, we also carried out off-normal studies in the c(2x2)Se/Ni(001) system. In Fig. 5a, we show results for emission into the ($\bar{1}$00) mirror plane at various polar angles, while in Fig. 5b similar data are shown for emission into the (0$\bar{1}\bar{1}$) mirror plane. The curves are rich in structure, and if they could be interpreted quantitatively, would probably yield

a good deal of information. It is also clear that the intensity modulations are not nearly as pronounced off normal as they are at normal emission. Indeed, at some angles little structure is observed at all. This can be undertood as arising from the reduction in symmetry of the off-normal final state and the consequent removal of degeneracies in the various time-reversed LEED beams contributing to the final state. We discussed this point earlier.[3] It is probably also responsible for smaller oscillations being observed in azimuthal spectra (APD). In contrast to the behavior of the LEED 00 beam,[14] there is no obvious systematic shift of peaks energies with (polar) emission angle. In fact the curves seem to evolve more by reduction in the intensities of some peaks and increases in others.

Although the off-normal curves in Fig. 5 were taken at a coarse angular mesh and do not represent as complete a study as would be desirable, as the first of their kind they yield enough information to merit several observations. Clearly the photoelectron diffraction curves evolve with polar angle θ differently than does a single LEED beam. This is, by negative inference, consistent with the expectation that the off-normal photoelectron diffraction curve will be comprised of a coherent superposition of several LEED beams, with the amplitude admixture coefficients varying with θ. Careful theoretical analysis will be required to establish the extent to which these curves can in fact be fitted quantitatively.

One of the original incentives for these off-normal studies
was to explore whether the intensity-voltage curves became par-
ticularly simple at particular non-zero values of Θ. For
example, the (Θ_{e-}, ϕ_{e-}) combinations of (45°, 180°) and (54°, 225°)
correspond to emission normal to the ($\bar{1}$01) and ($\bar{1}\bar{1}$1) planes,
respectively. Some sensitivity might be expected in these
curves to the $d_{\perp}$ values of overlayer selenium relative to these
two planes, although complicating factors abound; e.g., low
symmetry, energy-dependent refraction, etc. In fact we have
not noted any obvious relationships between the forms of the
off-normal curves in Fig. 5 and the known adsorbate-substrate
geometry. This question must be left open pending further
experimental and theoretical work. There is, however, one
unexpected feature of the off-normal curves that deserves com-
ment. The three lateral pairs of off-normal curves in Fig. 5 show
a fair degree of resemblance to one another. This is most
pronounced in the middle pair, which is also the off-normal
pair showing the largest photoelectron diffraction modulation.
In Fig. 6 these two curves are compared on a common energy
scale. Several of the most prominent peaks fall at similar
energies, with similar intensities, in the two curves. At this
point we can only note this interesting similarity as an
empirical fact, to be clarifed by further research. The pair-
wise similarity of the curves in Fig. 5 for similar polar but
different azimuthal angles suggests in a very tentative way
that the polar angle alone may be a critical variable in

determining the scattering curve. This would be true, for example, if the substrate surface were effectively an isotropic scattering plane.

Perhaps the most conclusive way to show that NPD does not simply measure the 00 LEED beam is to study a different system in which peak energies in the LEED 00 beam are similar to those in the selenium system, but for which peaks in the NPD curve are different. Such a system is c(2x2) sulfur on Ni(100). In Fig. 7 we show NPD results for that system and, for comparison, the second curve in Fig. 3 which shows similar data for the Se c(2x2)/Ni(001). The S(2p) core level was used as an initial state for the sulfur data. At first sight the curves in Fig. 7 appear remarkably similar. However, as the dashed lines in the figure and the tabulation of peak positions in Table II indicate, there are differences between the two cases which are well outside our experimental error and which cannot be removed by simply shifting one curve with respect to the other. The curves' similar appearance is probably attributable to the fact that the S(2p) and Se(3d) radial wave functions are similar; hence the atomic cross-section term discussed earlier will be similar for the two cases. Calculations will be presented in a future paper which will show that the sulfur data can be fitted using a value of $d_{\perp} = 1.3\text{Å}$,[15] the same value reported from LEED[7] and other photoemission analyses.[16] This result is the clearest indication that NPD is sensitive to $d_{\perp}$.

The final data set which we wish to present (Fig. 8) is that for disordered, low coverages of selenium on Ni(001). The top curve in Fig. 8 shows NPD data for a coverage of approximately 0.1 monolayer, while the middle curve is for 0.2 monolayer. Neither surface gave an ordered LEED pattern, but both show substantial photoelectron diffraction effects. Indeed, the amplitude of oscillation is nearly as large in these two cases as in the bottom curve, which shows the c(2x2) curve for comparison. The significance of this result should not be under-emphasized. It shows first that the dominant scattering mechanism in NPD is definitely off the substrate and not the overlayer itself; otherwise the effect in the disordered overlayer would not be so large. It also confirms the claim made in our earlier paper that NPD, like EXAFS, can deal quite effectively with disordered overlayer systems which are common in surface studies (especially in the case of stepped crystals). This is a significant advantage over LEED, in which 00 beam intensity variations are the only changes useful in making a structure determination on disordered overlayers. A similar experiment using azimuthal photoelectron diffraction is clearly in order, to determine the extent to which APD is sensitive to the substrate-adsorbate overlayer geometry as opposed to the geometry of the overlayer alone.

IV. CONCLUSIONS

In this paper we have reported the results of a series of experiments designed to test the viability of NPD as a surface structure-sensitive technique. Our principal conclusion is that NPD is indeed structure-sensitive, and is a candidate technique for adsorbate structure determinations. Detailed conclusions are given below.

1. Both adsorbate and substrate levels show large NPD oscillations, including multiple scattering peaks. Thus photoelectron difffraction effects, including multiple scattering, must be considered in quantiative interpretations of intensities in angle-resolved photoemission experiments.

2. NPD intensity-energy curves are reproducible, and peak positions show little sensitivity to the direction of the photon $\vec{A}$ vector.

3. The intensity-energy curves for both sulfur and selenium on Ni(001) behave like atomic cross-sections, modulated by photoelectron diffraction peaks, supporting a two-step mechanism.

4. NPD measures a coherent superposition of LEED beams, rather than the 00 beam alone. This follows both from off-normal studies of c(2x2)Se/Ni(001) and from NPD studies of c(2x2)S/Ni(001).

5. NPD is applicable to disordered adsorbate systems.

6. Off-normal curves showed smaller oscillation ampli-
tudes than NPD curves, and showed somewhat similar
evolution with Θ for two different values of ϕ.

ACKNOWLEDGEMENTS

Table I. NPD Peak Energies (in eV) for c(2x2)Se(3d)/Ni(001)

Data set[a]	Peak 1	Peak 2	Peak 3	Peak 4
3a	37[b]	53	86	130
3b	37	52	86	131
3c	37	52	89	136
3d	37	54	87	130

a) Refers to curves a - d in Fig. 3.
b) All entries are electron kinetic energies referred to
   the nickel vacuum level.

Table II. Comparison of NPD and LEED 00 Peak Energies.

c(2x2)S(2p)	NPD[a]	LEED 00[b]
Peak 1	32 eV	36
Peak 2	52 eV	56
Peak 3	78 eV	92
c(2x2)Se(3d)		
Peak 1	37 eV	39
Peak 2	52 eV	56
Peak 3	86 eV	91

a) All NPD data are electron kinetic energies
    referred to the nickel vacuum level.

b) All LEED data from Ref. 14.

REFERENCES

1. A. Liebsch, Phys. Rev. Lett. $\underline{32}$, 1203 (1974) and Phys. Rev. $\underline{B13}$, 544 (1976).

2. S. Y. Tong and M. A. Van Hove, Solid State Commun. $\underline{19}$, 543 (1976); S. Y. Tong and N. Stoner, J. Phys. $\underline{C11}$, 3511 (1978); S. Y. Tong and C. H. Li, Bull. Am. Phys. Soc. $\underline{23}$, 417 (1978).

3. S. D. Kevan, D. H. Rosenblatt, D. Denley, B.-C. Lu, and D. A. Shirley, Phys. Rev. Lett. $\underline{41}$, 1565 (1978).

4. G. J. Lapeyre, private communication, February, 1979.

5. S. Kono, C. S. Fadley, N.F.T. Hall, and Z. Hussain, Phys. Rev. Lett. $\underline{41}$, 117 (1978).

6. D. P. Woodruff, D. Norman, B. W. Holland, N. V. Smith, H. H. Farrell, and M. M. Traum, Phys. Rev. Lett. $\underline{41}$, 1130 (1978).

7. M. Van Hove and S. Y. Tong, J. Vac. Sci. Tech. $\underline{12}$, 230 (1975); S. Anderson, J. B. Pendry, B. Kasemo, and M. Van Hove, Phys. Rev. Lett. $\underline{31}$, 595 (1973).

8. (a) S. Y. Tong, private communication, October, 1978; (b) N. V. Smith, private communication, March, 1979.

9. H. D. Hagström and G. E. Becker, J. Chem. Phys. $\underline{54}$, 1015 (1971).

10. P. A. Sturrock, _Static and Dynamic Electron Optics_, Cambridge, 1955.

11. H.-J. Hagemann, W. Gudat, and C. Kunz, DESY Report SR-74/7, May, 1974 (unpublished).

12. D. A. Shirley, J. Stöhr, P. S. Wehner, R. S. Williams, and G. Apai, Physica Scripta $\underline{16}$, 398 (1977).

13. C. H. Li and S. Y. Tong, Phys. Rev. Lett. **42**, 901 (1979).

14. J. E. Demuth and T. N. Rhodin, Surf. Sci. **45**, 249 (1974).

15. S. Y. Tong, private communication, February, 1979.

16. C. H. Li and S. Y. Tong, Phys. Rev. Lett. **40**, 46 (1978).

FIGURE CAPTIONS

Figure 1. Normal photoemission spectrum from c(2x2)Se/Ni(001)
at the photon energy $h\nu$ = 150 eV, showing the nickel
valence band Se(3d), and Ni(3p) peaks. Note surface
sensitivity to 1/2 monolayer of Se.

Figure 2. Normal photoemission intensity versus kinetic energy
curves for (a) Ni(3p), (b) Se(3d), and (c) Ni valence
band electrons from p(2x2)Se/Ni(001), plotted as
intensity versus electron kinetic energy referenced
to the nickel vacuum level. Note diffraction maxima
at different energies on all curves.

Figure 3. Normal photoelectron diffraction curves for Se(3d)
electrons from c(2x2)Se/Ni(001), for different
samples and photon polarization vector orientations.

Figure 4. NPD curve for Se(3d) electrons from p(2x2)Se/Ni(001),
compared with theoretical curve by Li and Tong,[13]
and to LEED-beam curves by Demuth and Rhodin.[14]

Figure 5. Off-normal Se(3d) photoelectron diffraction curves
for the c(2x2)Se/Ni(001) system (a) in the ($\bar{1}$00)
mirror plane; (b) in the (0$\bar{1}\bar{1}$) mirror plane. Note
similarity of lateral pairs.

Figure 6. Direct comparison of the middle pair of off-normal
curves from Fig. 5. Note similarity of overall shape
and particularly of peaks near kinetic energies of 55,
111, and 184 eV.

Figure 7.　Comparison of NPD curves for c(2x2)S/Ni(001) and

　　　　　　c(2x2)Se/Ni(001).

Figure 8.　Comparison of NPD curves for Se(3d) in disordered

　　　　　　Se on Ni(001) at (a) 0.1 monolayer, (b) 0.2 mono-

　　　　　　layer, with the c(2x2) pattern.

c(2×2) Se/Ni(OOI)   hν =150 eV
Ni valence band
Se (3d)
Ni (3p)

Intensity (arbitrary units)

Binding energy (eV)
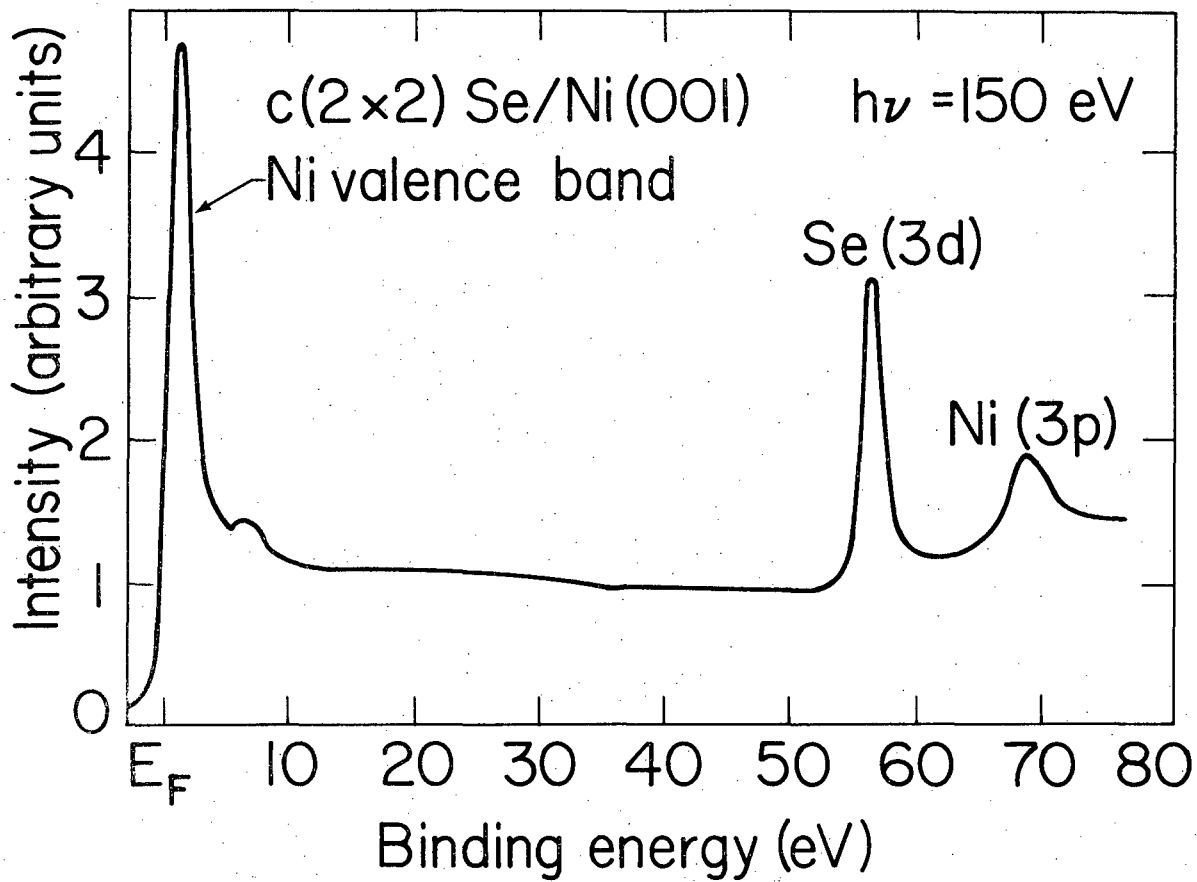
XBL 794-1372
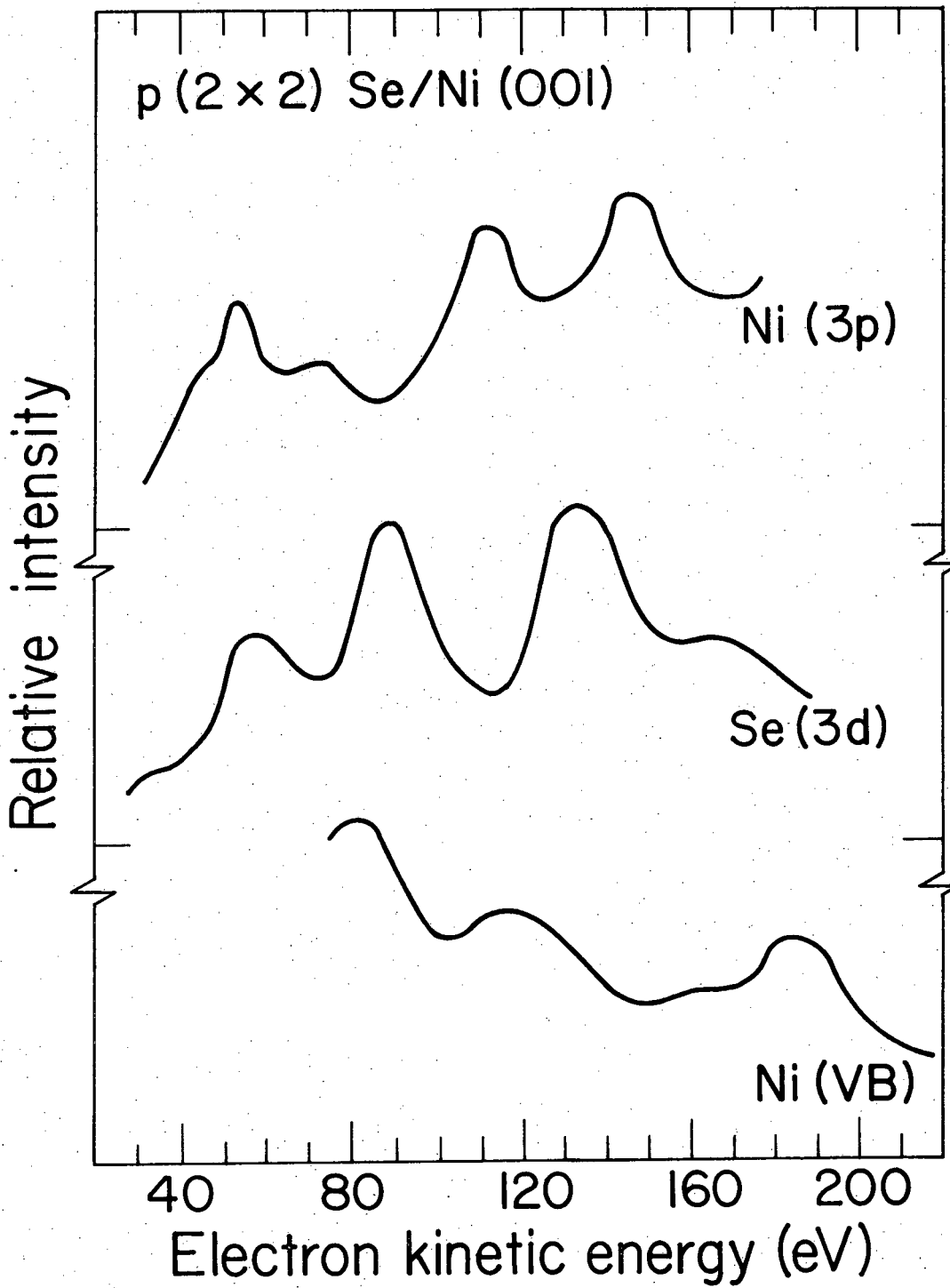
Figure 1

Figure 2
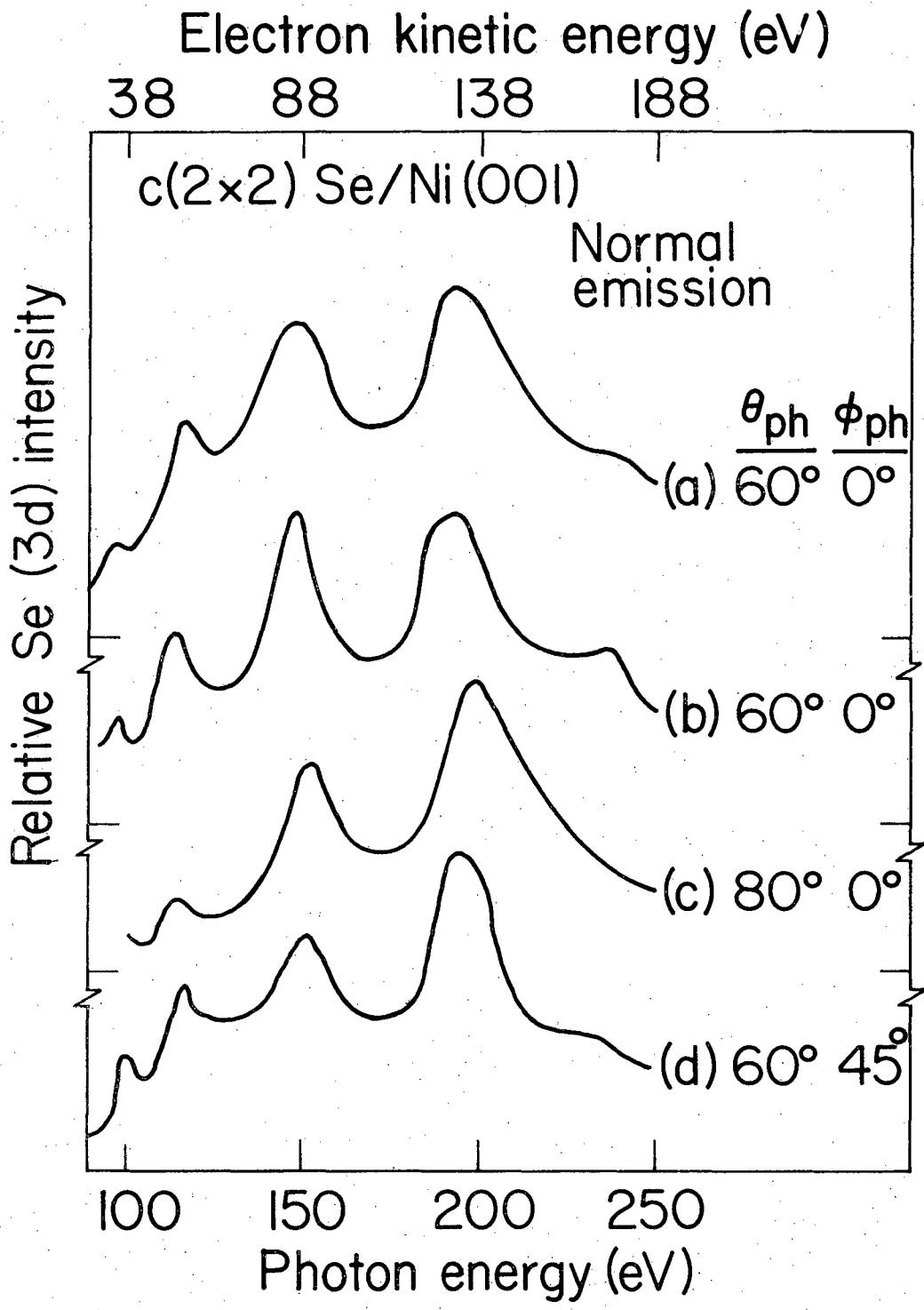
XBL 794-1374

Figure 3

XBL 794-1371
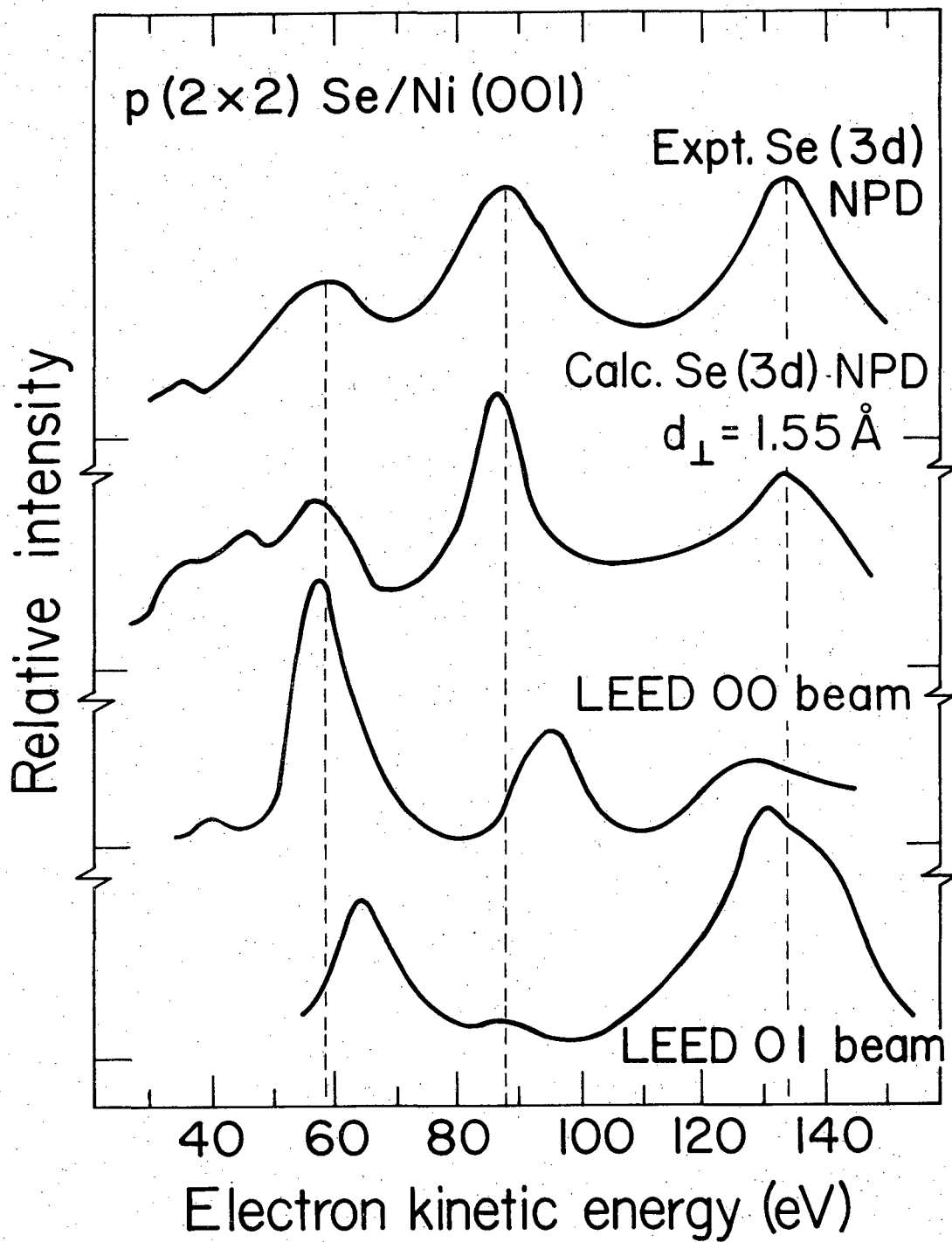
Figure 4

XBL 794-1373
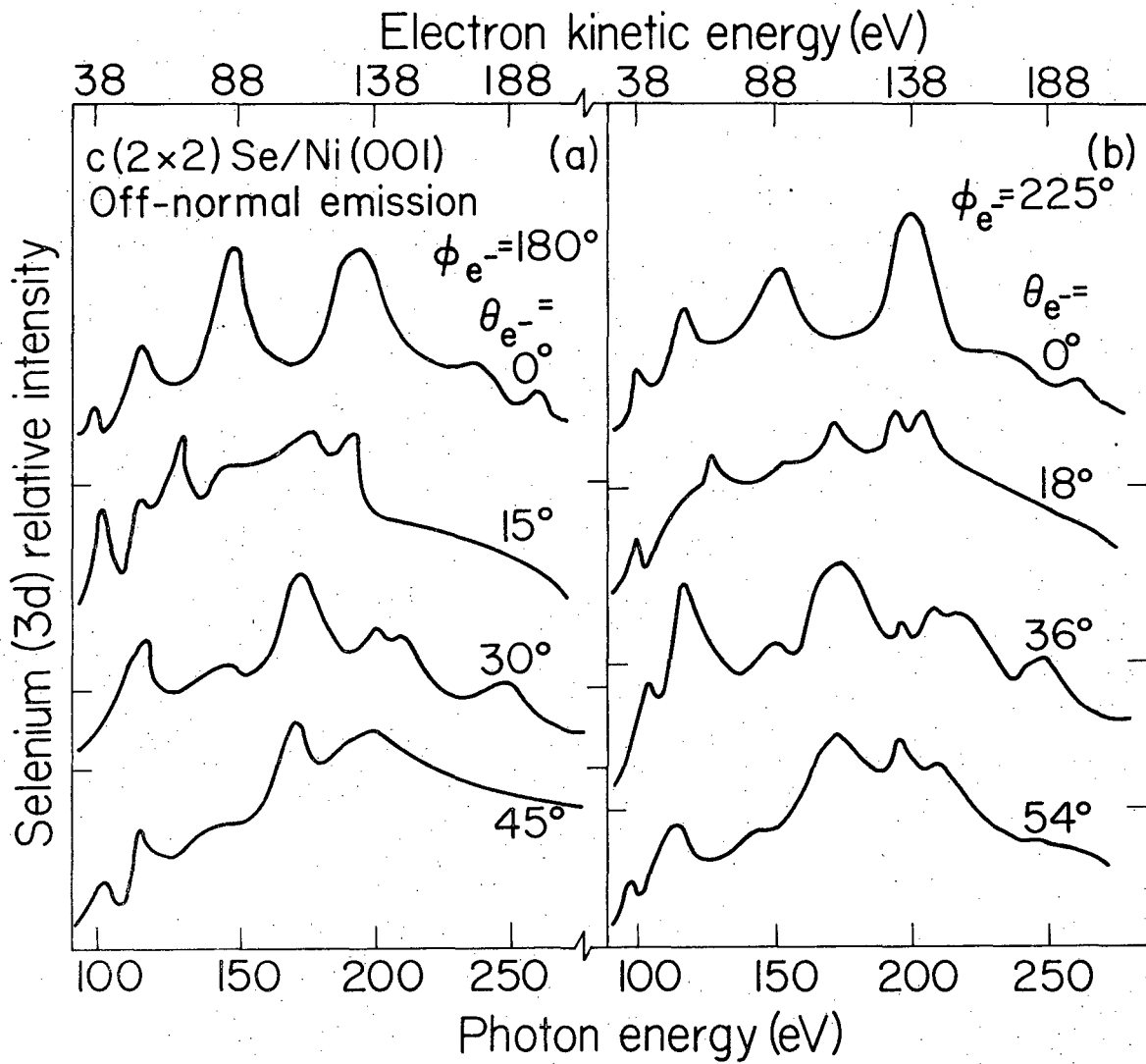
Figure 5

XBL 794-1370
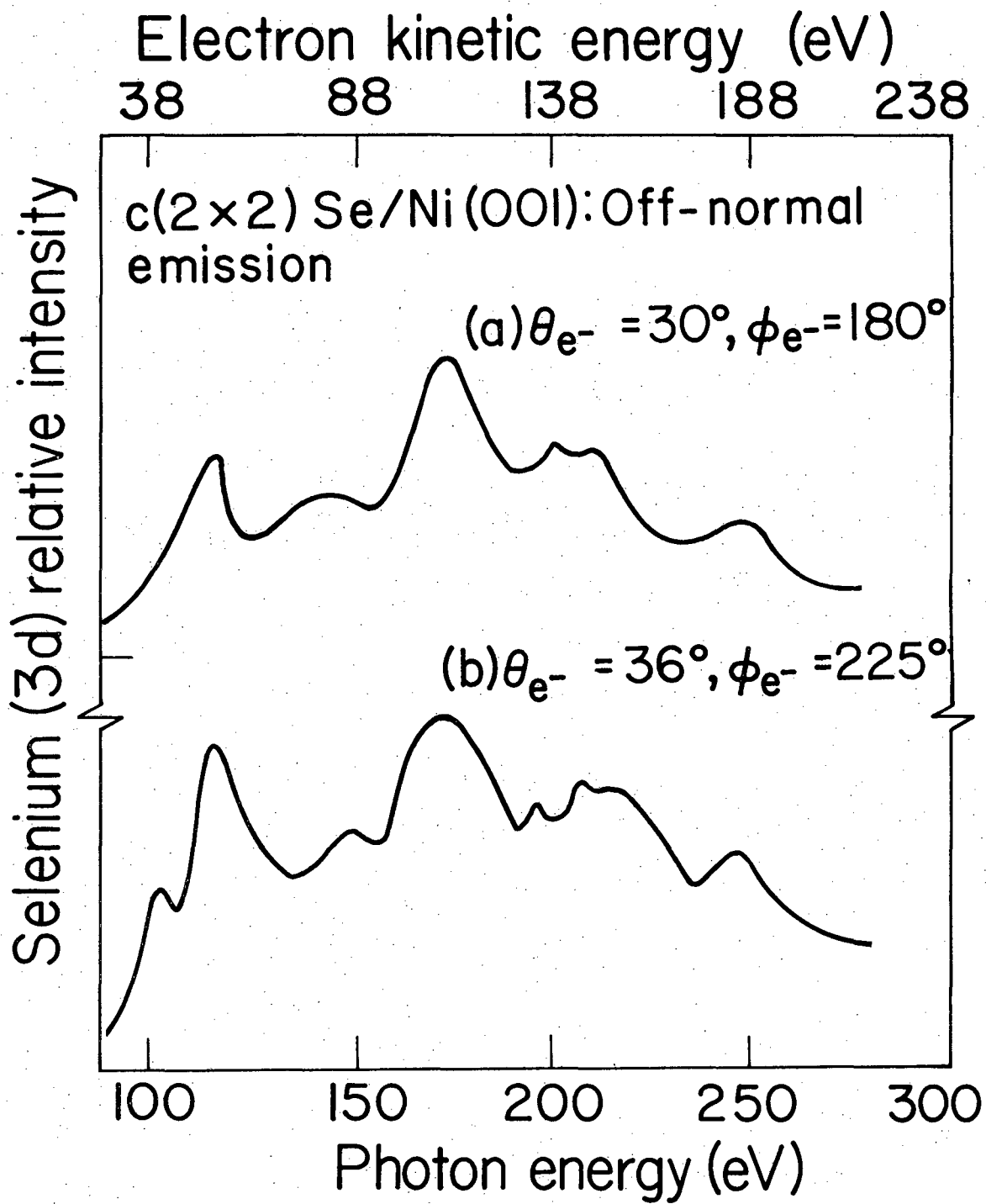
Figure 6

XBL 794-1369
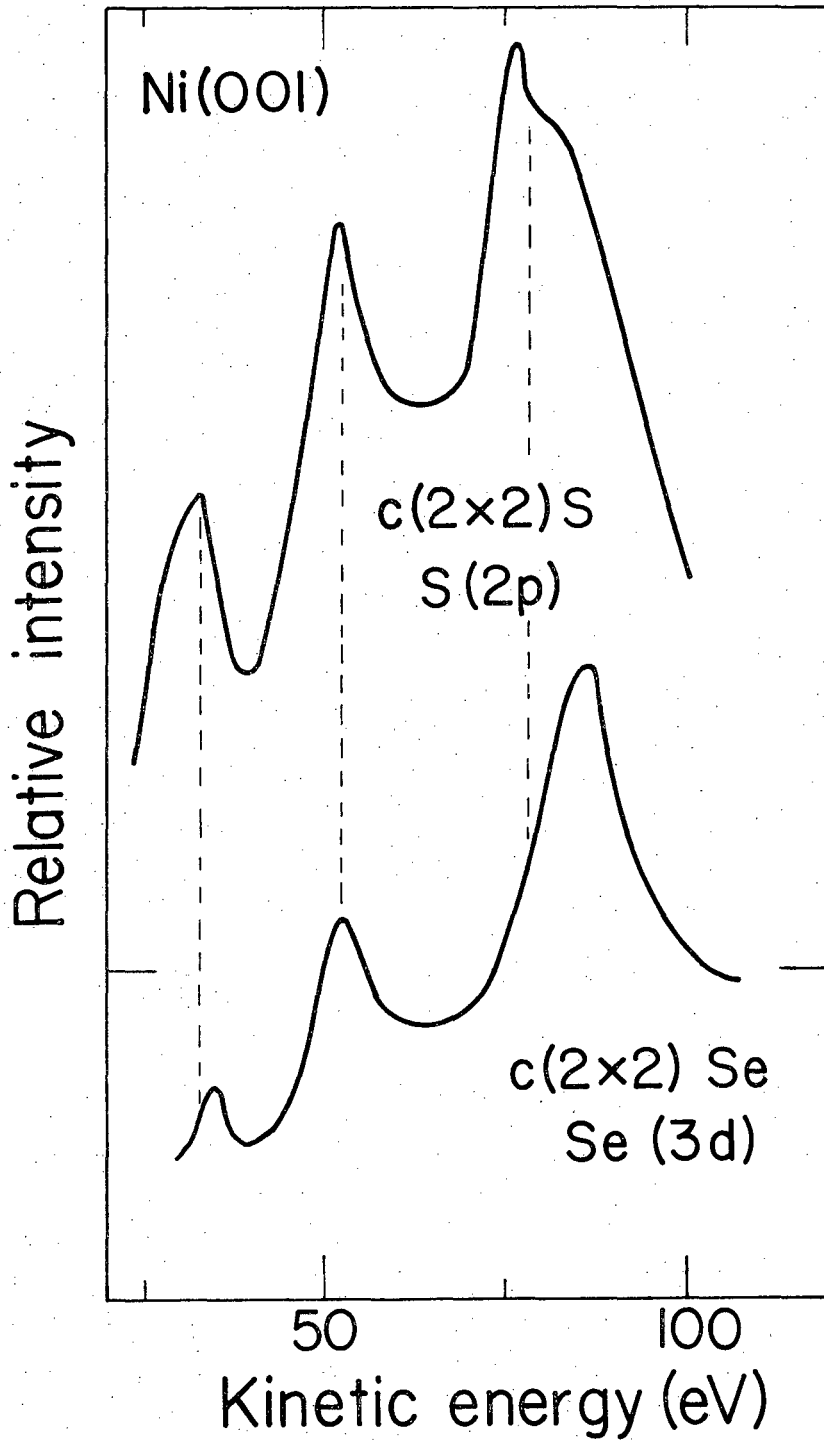
XBL 794-1375

Figure 7
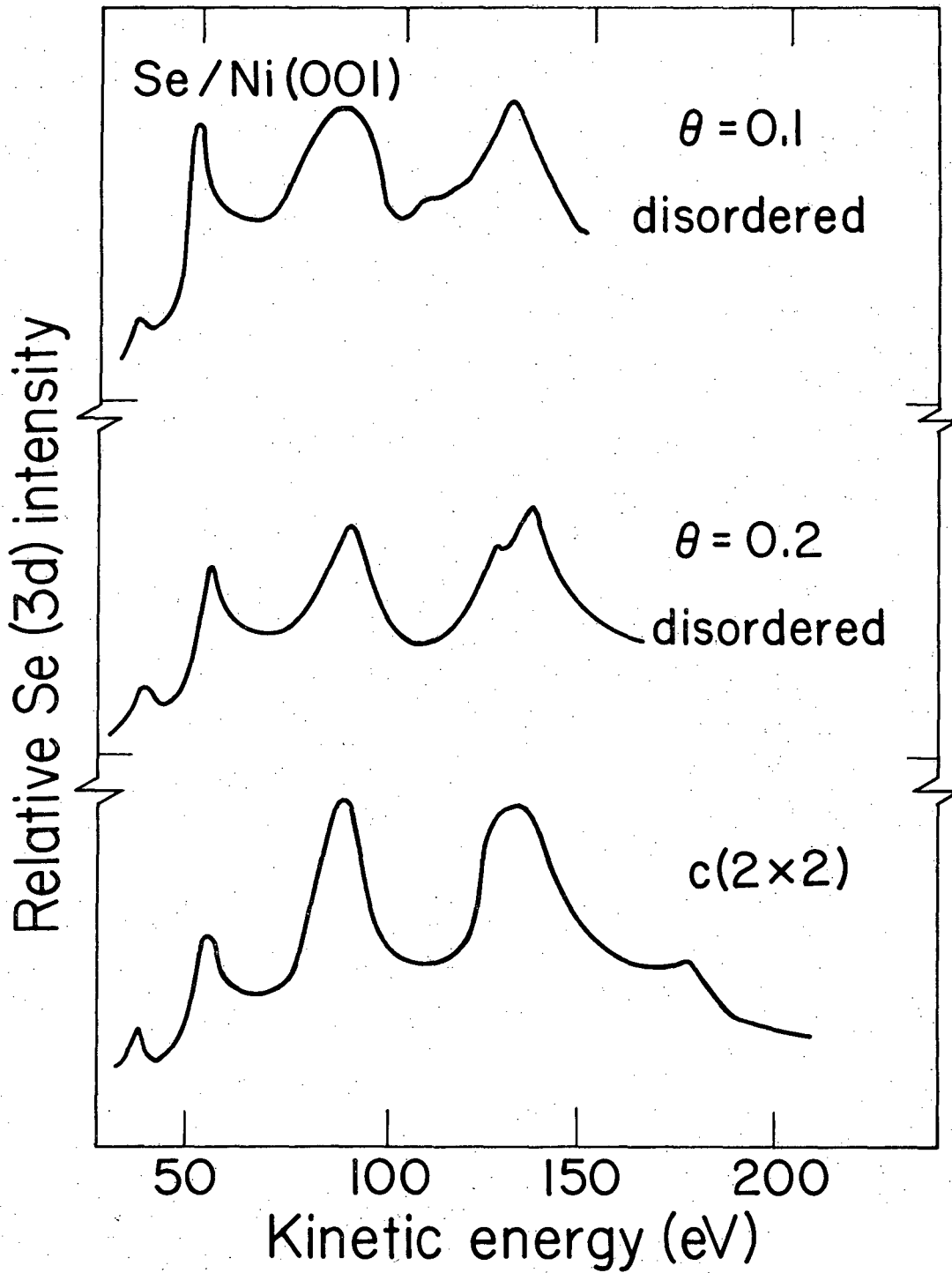
Figure 3   XBL 794-1376

TECHNICAL INFORMATION DEPARTMENT
LAWRENCE BERKELEY LABORATORY
UNIVERSITY OF CALIFORNIA
BERKELEY, CALIFORNIA 94720